



Cite this: *J. Mater. Chem. B*, 2017, 5, 5272

Facile synthesis of red-emitting carbon dots from pulp-free lemon juice for bioimaging†

Hui Ding,^a Yuan Ji,^a Ji-Shi Wei,^b Qing-Yu Gao,^a Zi-Yuan Zhou*^c and Huan-Ming Xiong^b

In this work, red-emitting carbon dots (R-CDs) with a high quantum yield (QY) of 28% in water were synthesized for the first time by heating an ethanol solution of pulp-free lemon juice. The obtained R-CDs were mono-dispersed with an average diameter of 4.6 nm, and exhibited excitation-independent emission at 631 nm. Meanwhile, these R-CDs featured low cytotoxicity and good photostability, which allow R-CDs to be employed as luminescent probes for *in vitro/in vivo* bioimaging. In addition, a detailed study on the physical properties and structural compositions of the sodium borohydride (NaBH₄) reduced R-CDs with orange emission suggested that surface states on the R-CD surfaces and nitrogen-derived structures in the R-CD cores synergistically caused their intense red luminescence. The low-cost and eco-friendly synthesis method and favorable optical properties of R-CDs make these carbon dots promising for further applications, such as bioimaging and light-emitting diodes.

Received 25th April 2017,
Accepted 1st June 2017

DOI: 10.1039/c7tb01130j

rsc.li/materials-b

Introduction

Over the past decade, carbon dots (CDs) have emerged as promising candidates for replacing traditional semiconductor quantum dots (QDs) and organic dyes because of inexpensive carbon sources, facile synthetic routes, unique physical properties, and extremely low toxicity.^{1–5} A vast number of carbon sources and synthetic methods have been developed to produce CDs for a wide range of applications, such as bioimaging, sensing, catalysis, full-color displays, and optoelectronic devices.^{6–9} However, most of the reported CDs emitted intense blue-green luminescence under excitation of ultraviolet (UV) light, and had relatively low quantum yields (QYs) in long wavelength ranges.^{10–12} These drawbacks seriously restricted their potential applications, especially in the field of bioimaging, because of strong tissue autofluorescence at low wavelength emissions and potential tissue damage due to ultraviolet light exposure.^{13–15} Thus, preparing long-wavelength emissive CDs excited by visible light with high quantum yields is of great importance.

To date, due to the unclear photoluminescence (PL) mechanism, only a few works have reported the successful preparation of CDs with long-wavelength emissions. For instance, Qu *et al.* synthesized highly efficient orange-emissive CDs with a photoluminescence (PL)

peak at 580 nm by heating a dimethylformamide solution of citric acid and urea.¹⁶ Fan *et al.* prepared red-emitting CDs (R-CDs) with a QY of 12% from the solvothermal treatment of citric acid and 1,5-diaminonaphthalene in an ethanol solution.¹⁷ In addition, Lin *et al.* produced red-luminescent CDs with a PL peak at 640 nm by heating a formamide solution of citric acid.¹⁸ Hu *et al.* also reported R-CDs with a QY as low as 6% in water through a complicated procedure.¹⁹ Although CDs with long-wavelength emissions have been obtained in these pioneering works, some critical limitations still exist, such as low QYs in water, the lack of pure red emission, sophisticated reaction processes, or time-consuming purification. Furthermore, large amounts of expensive or even toxic chemicals need to be used in these synthetic protocols, which is unbeneficial to the low-cost and eco-friendly synthesis of R-CDs for widespread application.²⁰ Therefore, developing facile methods that use renewable and low-cost biomass as a carbon source to synthesize R-CDs with beneficial optical properties and less environmental impact is highly needed.

Lemon juice, as a very common and inexpensive drink, contains vitamins, minerals and carbohydrates necessary for CD synthesis. In this work, we report a facile and eco-friendly synthesis of highly efficient R-CDs for the first time by the solvothermal heating of an ethanol solution of pulp-free lemon juice. The as-prepared R-CDs exhibit a PL peak at 631 nm and a QY of 28%, which is remarkable for red emissive CDs in water. The R-CDs were compared to the sodium borohydride (NaBH₄) reduced R-CDs using TEM, FTIR, XPS, UV and PL spectra in order to determine the PL origin for the intense red emission. The surface states and nitrogen-derived structures of CDs were

^a College of Chemical Engineering, China University of Mining and Technology, Xuzhou 221116, Jiangsu, P. R. China. E-mail: hding@cumt.edu.cn

^b Department of Chemistry and Shanghai Key Laboratory of Molecular Catalysis and Innovative Materials, Fudan University, Shanghai 200433, China

^c College of Science, China Agricultural University, Beijing 100193, China. E-mail: zhouziyuan@cau.edu.cn

† Electronic supplementary information (ESI) available. See DOI: 10.1039/c7tb01130j

determined to be synergistically responsible for the intense red luminescence of CDs. In addition, these R-CDs also show favorable excitation-independent PL, high photostability, stable dispersion in water, and lower toxicity compared to other CDs. These R-CDs can be successfully applied to *in vitro/in vivo* bioimaging by virtue of their strong red luminescence in a biological environment.

Experimental

Materials

Ethanol and ethyl acetate were purchased from Sinopharm Chemical Reagent Co. (China). Dulbecco's modified Eagle's medium (DMEM, High Glucose), fetal bovine serum (FBS), and trypsinase were obtained from Gibco BRL (USA). 3-(4,5-Dimethylthiazol-2-yl)-2,5-diphenyltetrazolium bromide (MTT) was acquired from Sigma-Aldrich. All chemical reagents were used as received. Ultrapure water (Milli-Q water) was used during the experiments. Pulp-free lemon juice, as shown in Fig. 1, was used as a carbon source for CD synthesis.

Characterization

A Tecnai G2 F20 transmission electron microscope operating at 200 kV was utilized for transmission electron microscopy (TEM) to capture high-resolution TEM images of R-CDs and r-CDs. The UV-Vis absorption spectra were collected using a PERSEE T10CS UV-Vis spectrometer with 1 cm path length quartz cuvettes. The fluorescence spectra were obtained on an F-4600 spectrofluorometer with excitation and emission slit widths of 2 nm and 2 nm, respectively. The FTIR spectra were obtained on a VERTEX 80v spectrometer. The Raman spectra were recorded using a Senterra Raman spectrometer at a 785 nm excitation wavelength. The X-ray photoelectron spectra were recorded using a D8 Advance spectrometer. The photoluminescence decay was measured on an FLS 920 spectrometer. *In vivo* mouse imaging experiments were successfully performed using a Bruker imaging system.

Synthesis of R-CDs

Twenty mL of pulp-free lemon juice was mixed with 10 mL of ethanol to form a transparent solution. Then, the mixture was transferred into a 100 mL Teflon-lined stainless-steel autoclave and heated at 190 °C for 10 hours. After the reaction was complete, the autoclave was cooled down naturally to room temperature. Subsequently, the resultant CD mixture was purified *via* silica column chromatography using a mixture of ethyl acetate and methanol as an eluent. Finally, R-CDs were obtained and then redispersed in water for further characterization.

Reduction of R-CDs

An excess amount of NaBH₄ was added to an R-CD aqueous solution and the mixture was stirred at room temperature for 4 h. Then, the mixture was transferred into a dialysis bag with a cut-off molecular weight of 1000 Da for dialysis against water for one day.

MTT assays

HeLa cells were seeded into a 96-well plate with a density of 1×10^5 cells per mL using Dulbecco's-modified Eagle's medium (DMEM) containing 10% FBS and incubated in a 5% CO₂ incubator at 37 °C for 24 h. Afterward, the culture medium was replaced with 200 μ L of DMEM containing various concentrations of the R-CDs, and the cells were cultured for another 48 h. At the end of the incubation, 20 μ L of 5 mg mL⁻¹ MTT solution was added into each well. After incubation for a further 4 h, the culture medium was removed, and 150 μ L of DMSO was then added to dissolve the MTT. Finally, the mixture was shaken for 15 min at room temperature, and the absorbance of each well at 492 nm was measured using an automatic ELISA analyzer (SPR-960). Control experiments without R-CDs were also performed. Each experiment was conducted five times, and the averaged data were presented.

Cell imaging

Cellular fluorescence images were captured using an FV10i laser scanning confocal microscope. In brief, 1.0 mL of HeLa cells in DMEM with a density of 5×10^4 cells per mL were seeded into 6-well culture plates and incubated at 37 °C in a 5% CO₂ incubator for 24 h. After incubation, the DMEM was discarded, and a mixture of R-CDs (20 μ g mL⁻¹) in DMEM was added to each well for 1 h of incubation. Finally, the cells were washed three times with a phosphate buffer solution to remove the free R-CDs and then fixed with 4% paraformaldehyde.

QY measurements

The quantum yield was tested using an integrating sphere that was attached to an F-4600 spectrofluorometer. First of all, the R-CD aqueous solution was diluted to an absorption intensity of below 0.1 at an optimal excitation wavelength of 533 nm. Then, this aqueous solution was added into a 1 cm fluorescence cuvette, placed in the integrating sphere and excited with 533 nm monochromatic light. The fluorescence spectra were collected in the ranges of 523–543 and 450–850 nm, respectively. Meanwhile, the same fluorescence spectra for pure water were also recorded

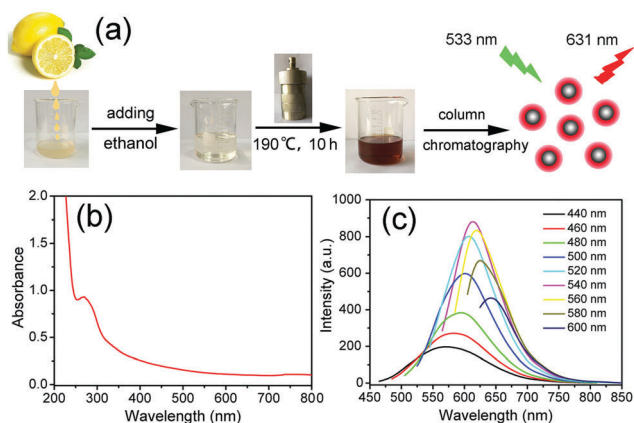


Fig. 1 (a) Illustration of the preparation process of the R-CDs from lemon juice by solvothermal treatment. (b) UV-visible absorption spectrum and (c) fluorescence spectra of the as-prepared CD mixtures excited by different wavelengths of light.

under identical conditions. Finally, the QYs were calculated using fluorescence software based on the PL spectra of both the sample and the water. Each experiment was conducted three times in parallel, and the QY values were averaged. Moreover, the QYs of the r-CD samples were measured using similar procedures, in which the recorded ranges were 491–511 nm and 400–810 nm, respectively, because the optimal excitation wavelength was 501 nm.

Results and discussion

As shown in Fig. 1a, the solvothermal treatment of pulp-free lemon juice at 190 °C for 10 hours yielded a dark brown-colored solution, which implied the generation of CDs.²¹ The UV-visible absorption spectra of the as-obtained mixture in Fig. 1b display an evident absorption band at 268 nm, with a tail almost crossing the entire visible light region. The fluorescence spectra in Fig. 1c show a typical excitation-dependent PL behavior, with a maximum at 615 nm. These unique optical properties imply that the resulting products were actually mixtures of CDs with different PL colors, and red luminescent CDs were dominant.²² Herein, it should be noted that ethanol is essential for the successful preparation of R-CDs because of an observation that repeating the reaction without adding ethanol to the lemon juice produces blue-emitting CDs (Fig. S1, ESI[†]). Subsequently, the as-prepared CD mixtures were purified using silica column chromatography. The R-CD fraction was collected and re-dispersed in water for further characterization.

Fig. 2a shows a transmission electron microscopy (TEM) image of the as-obtained R-CDs, revealing that these carbon dots were well monodispersed in water, with an average particle size of approximately 4.6 nm (Fig. S2, ESI[†]). The high-resolution TEM image presented in the inset displays a typical well-resolved crystal lattice with a spacing of 0.21 nm, representing the (100) in-plane lattice fringe of graphene.²³ The atomic force microscopy (AFM) image in Fig. 2b shows a thickness of about 1.5 nm, corresponding to 3 to 5 layers of graphene-like sheets.²⁴ The X-ray diffraction (XRD) pattern of the R-CDs, as shown in Fig. 2c, has an apparent peak at around 25° that is attributed to an interlayer spacing of 0.32 nm.²⁵ The Raman spectrum of these R-CDs in Fig. 2d reveals two peaks at 1344 cm⁻¹ (D band) and 1598 cm⁻¹ (G band), corresponding to areas of disorder or defects and sp² carbon networks in the carbon materials, respectively.^{26–28} The calculated intensity ratio I_D/I_G is 0.69, indicating a high degree of graphitization, which is consistent with the TEM and AFM results.

To further determine the structural compositions of the R-CDs, Fourier transform infrared (FT-IR) spectra and X-ray photoelectron spectra (XPS) were measured for the samples. In the FT-IR spectra (Fig. S3, ESI[†]), abundant hydrophilic groups, such as O–H at 3410 cm⁻¹, N–H at 3161 cm⁻¹, –COOH at 1705 cm⁻¹ and C–O at 1283 cm⁻¹, were observed for the R-CDs, which ensured their excellent solubility in water.^{29–32} Moreover, the FT-IR bands at 1591 and 1457 cm⁻¹, corresponding to C=C/C=N and C–N stretching vibrations, respectively, implied the formation of

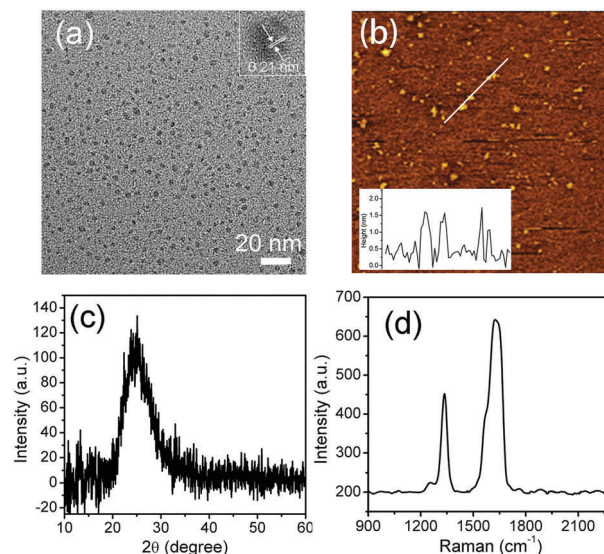


Fig. 2 (a) TEM and HRTEM (inset) images of the R-CDs. (b) AFM image of the R-CDs (inset: height profile along the line in (b)). (c) XRD pattern and (d) Raman spectrum of the R-CDs.

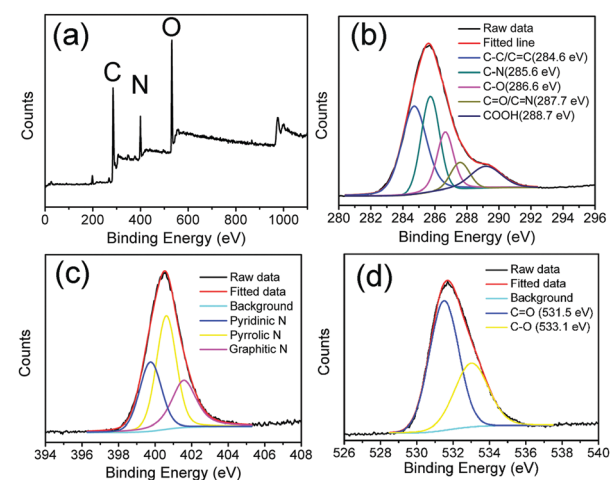


Fig. 3 (a) XPS spectrum and high-resolution (b) C1s, (c) N1s, and (d) O1s spectra of the R-CDs.

polyaromatic structures in the CD carbon cores.³³ The full XPS spectrum presented in Fig. 3a shows three typical peaks at 284, 400 and 531 eV, suggesting that the R-CD samples mainly consisted of C, N and O elements. Notably, the nitrogen content is up to 15% in our R-CD samples, much higher than that of many other reported red emissive CDs.^{34–37} In the high-resolution XPS spectra, the C1s band (Fig. 3b) can be deconvoluted into five peaks at 284.6, 285.6, 286.6, 287.7, and 288.7 eV, which correspond to C–C/C=C, C–N, C–O, C=O/C=N, and COOH, respectively. The N1s band (Fig. 3c) exhibits three peaks at 399.4, 400.6, and 401.5 eV, which are assigned to pyridinic C–N–C, pyrrolic C₂–N–H and graphitic N–C₃ groups, respectively. The O1s band in Fig. 3d contains two peaks at 531.5 and 533.1 eV for C=O and C–O, respectively. The C1s and N1s spectra clearly demonstrate the successful incorporation of

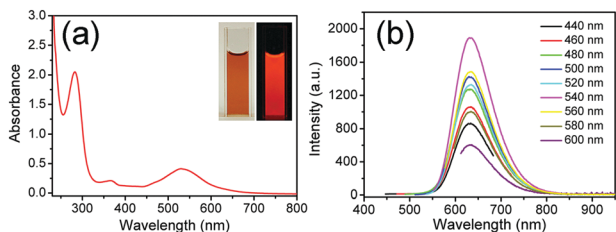


Fig. 4 (a) UV-visible absorption spectrum and (b) PL emission spectra of the as-obtained R-CDs under different excitation conditions. The inset contains photographs of the R-CD aqueous solution under daylight (left) and UV light (right).

nitrogen atoms into the core of the R-CDs.³⁸ On the basis of the aforementioned characterization data and analyses, it is confirmed that the R-CDs are composed of large π -conjugated domains in their cores and amorphous regions in their surfaces.

The optical properties of the R-CD samples were also investigated. In Fig. 4a, in the higher-energy UV region, the UV-visible absorption spectrum displays a noticeable peak at 271 nm, corresponding to the π - π^* transitions of the C=C bonds, which do not normally generate long-wavelength fluorescence.²⁵ However, in the lower-energy region from 300 to 600 nm, two new absorption bands at 371 and 538 nm are found, which are attributed to the n - π^* transitions of the C=O bonds and the surface states containing C=N/C=O and C-O structures,¹⁸ respectively. Such unique absorption features impart long-wavelength emission characteristics to the R-CDs. As shown in Fig. 4b, the PL spectra of the purified R-CDs exhibit an excitation-independent PL behavior, with a maximum emission peak at approximately 631 nm. Upon UV excitation at 365 nm, the R-CD aqueous solution immediately emits red-colored light (inset in Fig. 4a). When excited by an optimal excitation wavelength of 533 nm, the absolute QY of the R-CDs is measured to be approximately 28% by an integration sphere. Furthermore, the PL decay curves of the R-CDs (Fig. S4, ESI[†]) are fitted with a mono-exponential formula with a lifetime of 2.4 ns (Table S1, ESI[†]), which is close to those of other reported R-CDs.^{11,39} These distinct optical properties imply that our R-CDs possess uniform and excellent optical features after purification, which are quite different from those of the CD mixtures but in accordance with other previously reported CD fractions.⁴⁰

To date, the PL mechanisms of CDs have remained a matter of debate and many models have been proposed, including the quantum size effects, the band gaps based on multi-element doping and surface state controlled luminescence processes.^{1,8,41} In our previous research, PL tunable CDs from blue to red were obtained through a careful chromatography separation of CD mixtures synthesized in one-pot, and surface states, with increasing oxidation degree, were finally proven to be the main factor influencing their PL red shift.²² In the present work, to explore the origins of the intense red luminescence of the R-CDs samples, we synthesized four kinds of CD mixtures under the same reaction conditions except for adding different amounts of ethanol. After dialysis against water for one day, these purified CD mixtures were obtained and then characterized

to study the effects of the ethanol content added on the resulting CD mixtures. In Fig. S5 and S6 (ESI[†]), as the ethanol content increases, their PL spectra display a gradual PL redshift from 518 to 616 nm, while the TEM results exhibit no obvious changes in size, suggesting that the PL redshift may arise from the ethanol induced changes in structural compositions rather than from quantum size effects.²² These purified CD mixtures were further analyzed by using XPS to identify their structural compositions. As shown in Fig. S7 and Table S2 (ESI[†]), the nitrogen content increases from 10.3% to 12.4% with the PL redshift in CD mixtures, which indicates that ethanol facilitates the doping of nitrogen in the formation process of CDs and gives rise to changes in surface states.³⁶ It is known that a new surface state with a lower energy level can be formed on the CD surfaces after introduction of nitrogen, and thus red emissive CDs can be obtained by enhancing the nitrogen content in the CDs.⁴² To validate such a speculation, sodium borohydride (NaBH_4), a well-known reducing reagent, was utilized to reduce the surface states of the as-prepared R-CDs. After reduction and subsequent dialysis, the reduced R-CDs were obtained and then characterized. In Fig. 5a and b, these reduced R-CDs exhibit a similar average size of about 4.5 nm, implying that the surface reduction had no impact on their particle sizes. Meanwhile, an evident absorption decrease in the visible range is observed in the absorption spectrum of the reduced R-CDs (Fig. 5c), indicating that many surface groups like C=O and C=N were reduced, which is also demonstrated by the structural analyses of the reduced R-CDs in Fig. S8, S9 and Tables S3 and S4 (ESI[†]) (*i.e.*, nitrogen content: 15.4 to 14.2%; C=O/C=N content: 8.67 to 6.30%).⁴² The corresponding PL spectra in Fig. 5d also exhibit an excitation-independent emission behavior, with the PL peak blue shifting to 589 nm. Such results clearly suggest

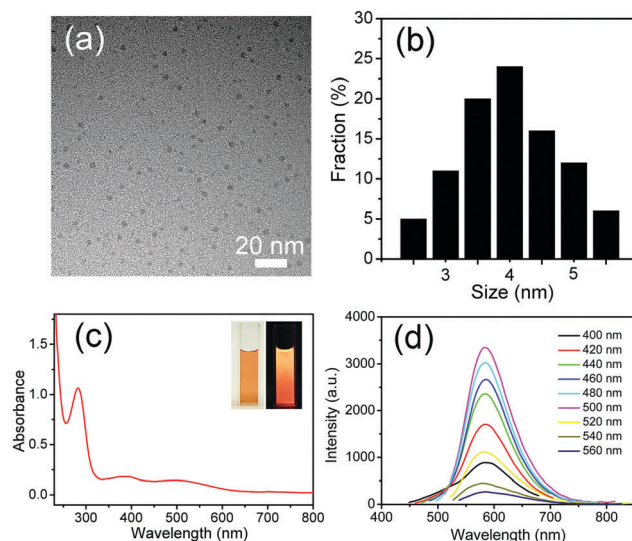


Fig. 5 (a) TEM image and (b) size distribution histogram of the NaBH_4 reduced R-CDs. (c) UV-visible absorption spectrum and (d) PL spectra of the NaBH_4 reduced R-CDs under different excitation wavelengths. The inset in (c) shows photographs of the reduced R-CD aqueous solution under daylight (left) and UV light (right).

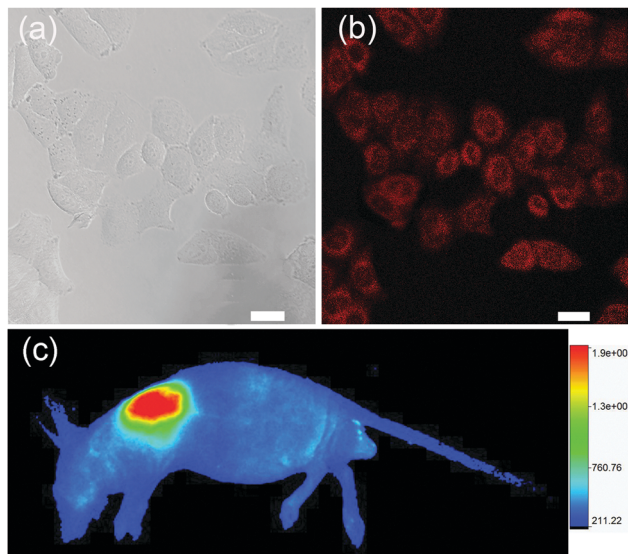


Fig. 6 Confocal fluorescence microscopy images of HeLa cells incubated with $20 \mu\text{g mL}^{-1}$ of the R-CDs for 1 h: (a) under a bright field and (b) under 514 nm excitation. (c) *In vivo* PL image of a nude mouse with subcutaneous injection of $100 \mu\text{L}$ of an aqueous solution of the R-CDs. The scale bar represents $25 \mu\text{m}$.

that surface states play a crucial role in controlling the red emissions of our R-CDs.¹⁰ In addition, besides the blue shifts of both the absorption and emission, our reduced R-CDs still possess a high QY up to 32% and about 14.2% nitrogen content after reduction, implying that nitrogen-derived structures, mainly in the form of pyrrolic N species or pyridinic N species, exist in their carbon cores and significantly influence the emission efficiency of the R-CDs.⁴³ Thus, according to our present analyses and other results in the literature, we believe the nitrogen-related surface states on CD surfaces and nitrogen-derived structures in carbon cores to be synergistically responsible for the intense red emission of our products.

Before the application of our R-CDs as red luminescent probes, the luminescence stability of the R-CD aqueous solutions at different pH values upon long-term UV irradiation was tested and the results were illustrated. In Fig. S10 (ESI[†]), the PL intensities decreased sharply in both strongly acidic and basic environments, while remaining about the same between pH values of 5 and 9, which is beneficial to practical applications in biological environments.⁴⁴ Likewise, the PL intensities show almost no attenuation after 1 hour of UV irradiation, suggesting that our R-CDs are quite stable against light irradiation (Fig. S11, ESI[†]). Subsequently, the cytotoxicity towards HeLa cells was measured using standard MTT assays. The results in Fig. S12 (ESI[†]) show that over 95% of the cells were still alive after incubation with $1000 \mu\text{g mL}^{-1}$ R-CDs for 48 h, which is less cytotoxic than many other reported CDs synthesized from chemicals.^{45–47} Thus, the R-CDs could be safely used for *in vitro* cell imaging. After incubation with $20 \mu\text{g mL}^{-1}$ of the R-CDs for 1 h, the HeLa cells could emit intense red fluorescence, mainly in the cytoplasm, under a laser confocal microscope (Fig. 6a and b), which further verifies the merits of our R-CDs. In addition, *in vivo*

mouse imaging was also performed. As shown in Fig. 6c, after subcutaneous injection of $100 \mu\text{L}$ of the R-CD aqueous solution, a strong PL signal with a good signal-to-noise ratio at the injection site can be observed under excitation and emission wavelengths of 535 nm 700 nm, respectively, which implies that the strong red PL can efficiently penetrate mouse skin and tissues.^{48–50} Furthermore, after the injections, the experimental animal gained about 1.2 g in weight in ten days, without any sign of acute toxicological responses (Fig. S13, ESI[†]), suggesting the excellent biocompatibility of our R-CDs. Taken together, these results demonstrate that the R-CDs can be used as a biocompatible and an effective luminescent probe for bio-imaging both *in vitro* and *in vivo*.

Conclusions

In summary, we have developed a straightforward, eco-friendly and low-cost method to produce highly red-luminescent CDs from pulp-free lemon juice. These R-CDs were well isolated from the CD mixture, and emitted bright, stable and excitation-independent red luminescence in aqueous solution. In addition, the R-CDs exhibited outstanding photostability and minimal cytotoxicity, which allowed them to be used as efficient red-emission agents for *in vitro/vivo* imaging. Moreover, the intense red luminescence of the R-CDs was demonstrated to have originated from their surface states and nitrogen-derived structures. This work provides a novel and inexpensive approach for the eco-friendly synthesis of high-quality red-emitting CDs from natural resources, and these R-CDs hold promise for biomedical and optoelectronic applications.

Acknowledgements

This work was financially supported by the Fundamental Research Funds for the Central Universities (No. 2017QNA08).

Notes and references

- 1 F. Yuan, S. Li, Z. Fan, X. Meng, L. Fan and S. Yang, *Nano Today*, 2016, **11**, 565–586.
- 2 R. Wang, K.-Q. Lu, Z.-R. Tang and Y.-J. Xu, *J. Mater. Chem. A*, 2017, **5**, 3717–3734.
- 3 P. G. Luo, S. Sahu, S.-T. Yang, S. K. Sonkar, J. Wang, H. Wang, G. E. LeCroy, L. Cao and Y.-P. Sun, *J. Mater. Chem. B*, 2013, **1**, 2116–2127.
- 4 Y. F. Wang and A. G. Hu, *J. Mater. Chem. C*, 2014, **2**, 6921–6939.
- 5 S. Y. Lim, W. Shen and Z. Gao, *Chem. Soc. Rev.*, 2015, **44**, 362–381.
- 6 S. Hu, *Chem. Rec.*, 2016, **16**, 219–230.
- 7 J. Wen, Y. Xu, H. Li, A. Lu and S. Sun, *Chem. Commun.*, 2015, **51**, 11346–11358.
- 8 A. Zhao, Z. Chen, C. Zhao, N. Gao, J. Ren and X. Qu, *Carbon*, 2015, **85**, 309–327.

- 9 X. M. Li, M. C. Rui, J. Z. Song, Z. H. Shen and H. B. Zeng, *Adv. Funct. Mater.*, 2015, **25**, 4929–4947.
- 10 S. Lu, L. Sui, J. Liu, S. Zhu, A. Chen, M. Jin and B. Yang, *Adv. Mater.*, 2017, **29**, 1603443.
- 11 K. Jiang, S. Sun, L. Zhang, Y. Lu, A. Wu, C. Cai and H. Lin, *Angew. Chem., Int. Ed.*, 2015, **54**, 5360–5363.
- 12 Z. Gan, H. Xu and Y. Hao, *Nanoscale*, 2016, **8**, 7794–7807.
- 13 L. Pan, S. Sun, L. Zhang, K. Jiang and H. Lin, *Nanoscale*, 2016, **8**, 17350–17356.
- 14 Y. B. Song, S. J. Zhu and B. Yang, *RSC Adv.*, 2014, **4**, 27184–27200.
- 15 H. Tao, K. Yang, Z. Ma, J. Wan, Y. Zhang, Z. Kang and Z. Liu, *Small*, 2011, **8**, 281–290.
- 16 S. Qu, D. Zhou, D. Li, W. Ji, P. Jing, D. Han, L. Liu, H. Zeng and D. Shen, *Adv. Mater.*, 2016, **28**, 3516–3521.
- 17 F. Yuan, Z. Wang, X. Li, Y. Li, Z. A. Tan, L. Fan and S. Yang, *Adv. Mater.*, 2017, **29**, 1604436.
- 18 S. Sun, L. Zhang, K. Jiang, A. Wu and H. Lin, *Chem. Mater.*, 2016, **28**, 8659–8668.
- 19 S. Hu, A. Trinchì, P. Atkin and I. Cole, *Angew. Chem., Int. Ed.*, 2015, **54**, 2970–2974.
- 20 L. Wang and H. S. Zhou, *Anal. Chem.*, 2014, **86**, 8902–8905.
- 21 Y. Li, X. Zhong, A. E. Rider, S. A. Furman and K. Ostrikov, *Green Chem.*, 2014, **16**, 2566.
- 22 H. Ding, S. B. Yu, J. S. Wei and H. M. Xiong, *ACS Nano*, 2016, **10**, 484–491.
- 23 M. X. Gao, C. F. Liu, Z. L. Wu, Q. L. Zeng, X. X. Yang, W. B. Wu, Y. F. Li and C. Z. Huang, *Chem. Commun.*, 2013, **49**, 8015–8017.
- 24 Z. Liang, L. Zeng, X. Cao, Q. Wang, X. Wang and R. Sun, *J. Mater. Chem. C*, 2014, **2**, 9760–9766.
- 25 H. Ding, J. S. Wei and H. M. Xiong, *Nanoscale*, 2014, **6**, 13817–13823.
- 26 X. Teng, C. Ma, C. Ge, M. Yan, J. Yang, Y. Zhang, P. C. Morais and H. Bi, *J. Mater. Chem. B*, 2014, **2**, 4631–4639.
- 27 Y. Dong, J. Lin, Y. Chen, F. Fu, Y. Chi and G. Chen, *Nanoscale*, 2014, **6**, 7410–7415.
- 28 P. Yang, J. Zhao, J. Wang, B. Cao, L. Li and Z. Zhu, *J. Mater. Chem. A*, 2015, **3**, 136–138.
- 29 H. He, X. Wang, Z. Feng, T. Cheng, X. Sun, Y. Sun, Y. Xia, S. Wang, J. Wang and X. Zhang, *J. Mater. Chem. B*, 2015, **3**, 4786–4789.
- 30 Q. Lu, J. Deng, Y. Hou, H. Wang, H. Li, Y. Zhang and S. Yao, *Chem. Commun.*, 2015, **51**, 7164–7167.
- 31 A. Cayuela, M. L. Soriano, C. Carrillo-Carrion and M. Valcarcel, *Chem. Commun.*, 2016, **52**, 1311–1326.
- 32 C. Li, F. Li, T. Li, T. Bai, L. Wang, Z. Shi and S. Feng, *Dalton Trans.*, 2012, **41**, 4890–4895.
- 33 J. Zhou, Y. Yang and C. Y. Zhang, *Chem. Commun.*, 2013, **49**, 8605–8607.
- 34 J. Ge, Q. Jia, W. Liu, L. Guo, Q. Liu, M. Lan, H. Zhang, X. Meng and P. Wang, *Adv. Mater.*, 2015, **27**, 4169–4177.
- 35 B. P. Jiang, B. Zhou, X. C. Shen, Y. X. Yu, S. C. Ji, C. C. Wen and H. Liang, *Chem. – Eur. J.*, 2015, **21**, 18993–18999.
- 36 L. Guo, J. Ge, W. Liu, G. Niu, Q. Jia, H. Wang and P. Wang, *Nanoscale*, 2015, **8**, 729–734.
- 37 C. Wang, K. Jiang, Q. Wu, J. Wu and C. Zhang, *Chem. – Eur. J.*, 2016, **22**, 14475–14479.
- 38 D. Qu, M. Zheng, L. Zhang, H. Zhao, Z. Xie, X. Jing, R. E. Haddad, H. Fan and Z. Sun, *Sci. Rep.*, 2014, **4**, 5294.
- 39 L. Bao, C. Liu, Z. L. Zhang and D. W. Pang, *Adv. Mater.*, 2015, **27**, 1663–1667.
- 40 J. C. Vinci and L. A. Colon, *Anal. Chem.*, 2012, **84**, 1178–1183.
- 41 S. Zhu, Y. Song, X. Zhao, J. Shao, J. Zhang and B. Yang, *Nano Res.*, 2015, **8**, 355–381.
- 42 H. Nie, M. Li, Q. Li, S. Liang, Y. Tan, L. Sheng, W. Shi and S. X.-A. Zhang, *Chem. Mater.*, 2014, **26**, 3104–3112.
- 43 Z. Qian, J. Ma, X. Shan, H. Feng, L. Shao and J. Chen, *Chem. – Eur. J.*, 2014, **20**, 2254–2263.
- 44 F. Li, C. Li, X. Liu, Y. Chen, T. Bai, L. Wang, Z. Shi and S. Feng, *Chem. – Eur. J.*, 2012, **18**, 11641–11646.
- 45 X. Tan, Y. Li, X. Li, S. Zhou, L. Fan and S. Yang, *Chem. Commun.*, 2015, **51**, 2544–2546.
- 46 W. Q. Kong, R. H. Liu, H. Li, J. Liu, H. Huang, Y. Liu and Z. H. Kang, *J. Mater. Chem. B*, 2014, **2**, 5077–5082.
- 47 A. Sachdev, I. Matai and P. Gopinath, *RSC Adv.*, 2014, **4**, 20915–20921.
- 48 F. Li, C. Li, J. Liu, X. Liu, L. Zhao, T. Bai, Q. Yuan, X. Kong, Y. Han, Z. Shi and S. Feng, *Nanoscale*, 2013, **5**, 6950–6959.
- 49 F. Li, C. Li, X. Liu, T. Bai, W. Dong, X. Zhang, Z. Shi and S. Feng, *Dalton Trans.*, 2013, **42**, 2015–2022.
- 50 F. Wu, H. Su, X. Zhu, K. Wang, Z. Zhang and W.-K. Wong, *J. Mater. Chem. B*, 2016, **4**, 6366–6372.